Chemical Physics Letters 640 (2015) 72–76

Contents lists available at ScienceDirect

Chemical Physics Letters

journal homepage: www.elsevier.com/locate/cplett

A diamond (1 0 0) surface with perfect phase purity

Oleksiy Dyachenko[a,*], Nadine Diek[a,b], Yevgeniy Shapiro[c], Rajesh Tamang[a], Wolfgang Harneit[c], Michael Reichling[a,*], Andriy Borodin[a]

[a] Fachbereich Physik, Universität Osnabrück, Barbarastr. 7, 49076 Osnabrück, Germany
[b] Institut für Chemie neuer Materialien, Barbarastr. 7, 49076 Osnabrück, Germany
[c] Institut für Physikalische Chemie, Johannes Gutenberg Universität Mainz, Duesbergweg 10–14, 55099 Mainz, Germany

ARTICLE INFO

Article history:
Received 18 August 2015
In final form 7 October 2015
Available online 22 October 2015

ABSTRACT

Diamond surfaces with (1 0 0) orientation and perfect phase purity regarding the coexistence of sp^3 and sp^2 bonding as well as near surface nitrogen implanted layers are repeatedly produced from one sample by a cycle of nitrogen implantation, etching in oxygen and wet chemical etching. Comprehensive surface studies carried out by X-ray photoelectron spectroscopy (XPS) involving a deconvolution of the C 1s peak into contributions of C sp^3, C sp^2 and C sp^3(N) reveal the surface and near-surface phase and stoichiometry. It is demonstrated that efficient etching of nitrogen implanted diamond occurs by high temperature annealing in oxygen and a wet chemical treatment.

1. Introduction

Outstanding electrochemical and defect properties of diamond make it an attractive material for a wide range of potential applications like quantum computing [1–4], electrochemical [5–7] and biochemical applications [8,9] where diamond surface properties play a paramount role. Diamond based electronic devices like high-power switching devices and radiation sensors [8,10] as well as applications where diamond is used as a substrate [11] for subsequent deposition of diamond or another material [12–16] require a full understanding of the surface state and full control over surface chemistry and treatment procedures. Surface functionalization [17] is important for the use of diamond in biomedical applications [18–20] and applications of diamond in quantum computing require a controlled near-surface doping of the sample with nitrogen to couple a spin system to nitrogen vacancy (NV) centres in diamond [21–23], while water layers and surface graphitization result in a severe degradation of the system functionality [8,24].

Therefore, the characterization of diamond with regard to surface morphology and topography [25], optical properties [26], mechanical properties [8] as well as electrical and thermal conductivity properties [8] has been addressed in various context. Specifically, X-ray photoelectron spectroscopy (XPS) has been applied for the characterization of nitrided [27], oxidized [28,29], etched [30] and clean [31] diamond surfaces and CVD diamond films via annealing in oxygen [32]. Furthermore, it has been shown that high temperature annealing of diamond [33], argon sputtering [30] and heavy ion bombardment [34] results in diamond surface amorphisation identified in XPS by a rise of the carbon sp^2 signal. Despite these strong efforts, a unified approach for the controlled preparation and characterization of diamond surfaces in different phase states is still missing.

Here, we focus on the precise characterization after different preparation steps to develop an optimum surface treatment procedure for diamond (1 0 0) with highest phase purity that can repetitively be prepared from the same crystal. The initial surface treatment is mechanical polishing while the repetitive steps of surface preparation sketched in Figure 1 comprise three simple physical and chemical treatments, namely ion implantation and annealing in ultra-high vacuum (UHV), annealing in an oxygen atmosphere and wet chemical etching. XPS results show that a phase purity of 88% sp^3 can be achieved. We further demonstrate that relicts from a shallow implantation of nitrogen can completely be removed by the described procedure so that the surface exhibits also an excellent stoichiometric purity.

2. Experimental

We use CVD grown diamond samples with a size of 3 mm × 3 mm × 0.5 mm and (1 0 0) surface orientation. The nitrogen concentration of the type IIa material is specified by the manufacturer (Element Six Ltd., Ascot, United Kingdom) to be below 1 ppm. Initial steps of surface preparation carried out by

* Corresponding authors.
E-mail addresses: odyachen@uos.de (O. Dyachenko), reichling@uos.de (M. Reichling).

http://dx.doi.org/10.1016/j.cplett.2015.10.015
0009-2614/

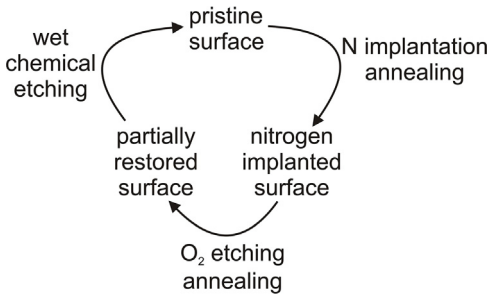

Figure 1. Cycle scheme for repetitive preparation of the diamond surface.

the manufacturer comprise mechanical polishing yielding a roughness of typically Ra < 30 nm and boiling in a strongly oxidizing acid solution composed of H_2SO_4 and KNO_3. The laboratory treatment starts with rinsing the surface with HPLC grade ethanol and dry wiping with an optical paper. After transferring the sample into the UHV chamber having a base pressure below 8×10^{-11} mbar, it is flashed to a temperature of 790 °C for 3 min to remove volatile adsorbates like water and hydrocarbons. All subsequent preparation steps and further measurements are performed in situ in the UHV environment except for the final step of wet chemical etching. The surface analysis after wet chemical etching is performed after re-transferring the sample into the UHV and is preceded by the same thermal treatment as used for initial surface cleaning.

To implant nitrogen and to create defects in a surface layer, the diamond sample is exposed for 60 s to a beam of nitrogen ions having 500 eV kinetic energy provided by a conventional sputter cleaning ion source, namely the Dual Filament Gun Model 981-2043 (Varian, Palo Alto, CA, USA) and flashed to a temperature of 790 °C to stabilize a certain concentration of nitrogen defect centres. Sample heating is accomplished by electron bombardment of a piece of Ta sheet metal attached to the diamond sample back side; the temperature is measured by a type K thermocouple attached to the Ta plate near the sample. The following step is annealing the sample in molecular oxygen (Messer Griesheim GmbH, Krefeld, Germany, O_2 purity better than 99.998%) at a pressure of 1.33×10^{-7} mbar. The sample is annealed in oxygen in many steps of 2 h duration to track changes induced by this treatment; the total annealing time is 27 h. The final step of preparation is wet chemical etching in a 1:1:1 acid mixture of H_2SO_4, HNO_3 and $HClO_4$ for 4 h at a temperature of 359 ± 2 °C and rinsing in Type I purified laboratory water (Arium 611UV, Sartorius AG, Goettingen, Germany).

After each treatment and annealing step, the sample is analyzed by XPS performed with a setup consisting of a X-ray source XR 50 (SPECS Surface Nano Analysis GmbH, Berlin, Germany) and a hemispherical electron energy analyser PHOIBOS 100 (SPECS Surface Nano Analysis GmbH, Berlin, Germany) equipped with a five channeltron assembly detector maintaining a high detection sensitivity at an energy resolution of 0.2 eV. Photoelectron spectra are taken using non-monochromatic radiation from the Al Kα and Mg Kα lines with photon energies of 1486.6 eV and 1253.6 eV, respectively. The X-rays are directed onto the sample under an angle of 30° while electrons emitted perpendicular from the surface are collected by the transfer optics of the electron analyser. Electrons are collected from an area having a diameter of 2 mm while the XPS sampling depth is about 3 nm (for Mg Kα radiation) yielding a sampling volume of about 10 000 μm^3. The sample is heated to a temperature of 350 °C during XPS measurements to yield some electrical conductivity avoiding surface charging. A typical survey spectrum obtained after the initial cleaning step yielding the pristine surface is shown as the black line in Figure 2. The main features are the C 1s and O 1s lines, the former having satellite and plasmon side bands. The presence of the oxygen core-level peak O 1s

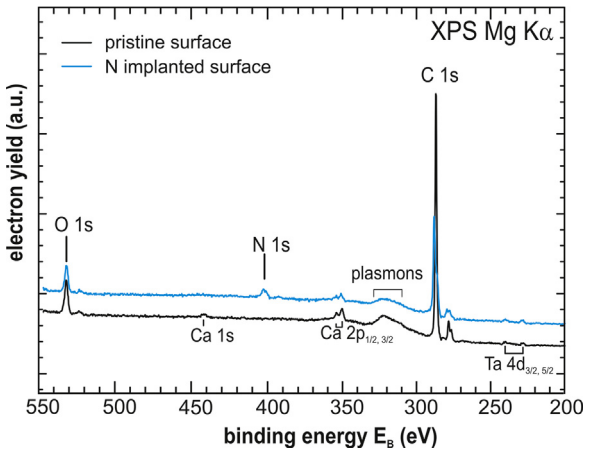

Figure 2. XPS survey spectra of the diamond surface in two states of preparation. The black curve shows a typical result for the pristine surface while the blue curve represents the result after nitrogen implantation. The minute signal of the Ta 4d line is due to emission from the Ta sample holder assembly while the origin of a small Ca signal present in almost all spectra is not clear; we suspect a contamination from trace impurities in surface cleaning agents applied after mechanical polishing. (For interpretation of the references to colour in this figure legend, the reader is referred to the web version of this article.)

indicates partial oxidation of the surface and is associated to a surface chemisorbed oxygen species. It is important to note that the O 1s peak at a binding energy of 532.2 eV decreases after flashing to 790 °C, however, the main part of the O 1s emission at 531.2 eV remains.

3. Results and discussion

To damage the surface and near surface layers in a controlled way and to study effects of nitrogen doping, the sample is exposed to nitrogen ions as described above. The resulting XPS survey spectrum shown as the blue curve in Figure 2 exhibits a small but verifiable N 1s signal indicating nitrogen implantation. To further explore the impact of nitrogen bombardment, two spectral regions of the photoemission spectrum are investigated in detail with results shown in Figures 3 and 4. The comparison of spectra

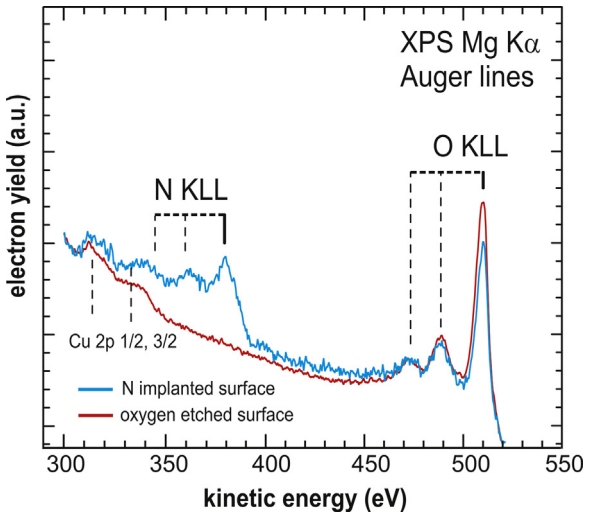

Figure 3. XPS Auger line analysis in the region of the N KLL and O KLL lines. The blue curve shows the result for the nitrogen implanted surface while the red curve demonstrates the complete removal of nitrogen after 27 h of etching in oxygen. The small Cu signal is ascribed to stray electrons emitted from parts made of copper at the nose of the X-ray source. (For interpretation of the references to colour in this figure legend, the reader is referred to the web version of this article.)

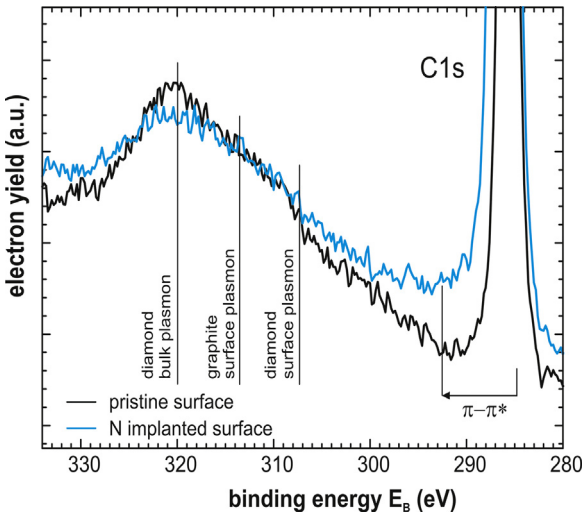

Figure 4. XPS detail spectrum in the vicinity of the C 1s peak. The black curve shows the result for the pristine surface while the blue curve represents the result after nitrogen implantation. (For interpretation of the references to colour in this figure legend, the reader is referred to the web version of this article.)

shown in Figure 3 is a confirmation of the nitrogen implantation evidenced by the presence of significant N KLL Auger lines. The analysis of Auger lines allows for a much more sensitive detection of nitrogen than analysing the XPS spectrum and here yields clear evidence that we are able to completely remove the nitrogen implanted layer by etching the surface in an oxygen atmosphere (in the following preparation step). The surface damage is evident from a detailed analysis of the diamond and graphite plasmon regions as shown in Figure 4. We find that a significant π–π^* transition loss peak appears after nitrogen implantation [35]. As this peak results from inelastic processes related to unoccupied π^* states at the surface, we attribute the peak to the formation of sp^2 carbon, for instance, amorphous carbon in the surface layer. The peak associated with the diamond bulk plasmon is due to a loss of energy from the departing core electrons to the bulk valence band and is shifted by 34 eV while the diamond surface plasmon is shifted by 22 eV relative to the C 1s peak [36]. The apparent drop of the intensity for the diamond bulk plasmon occurring upon nitrogen implantation yields further evidence for the transformation of diamond into sp^2 carbon.

The major conclusions drawn from the work reported here are based on a line shape analysis of the C 1s peak allowing for an identification of different spectral components in each state of preparation as shown in Figure 5. The analysis comprises the identification of a chemical shift due to the conversion of sp^3 to sp^2 carbon but also a shift of the sp^3 peak due to the presence of nitrogen further on denoted as sp^3(N). It is important to note that the sp^3 and sp^3(N) peaks coexist in certain steps of preparation due to inhomogeneity within the XPS sampling volume.

The basic step of the spectral deconvolution is the standard Shirley background subtraction. For fitting the C 1s line, the following single peak Gaussian/Lorentzian sum formula [35,37,38]

$$\mathrm{SPGL}(E) = y_0 \left\{ \frac{m}{1+((E-E_0)^2/\Delta E^2)} + (1-m)\exp\left[-\ln 2\left(\frac{(E-E_0)^2}{\Delta E^2}\right)\right]\right\}$$

is used for each spectral component with centre energy E_0, width ΔE and maximum yield y_0. As the natural line width of the C 1s component is large, for our instrumentation in the current

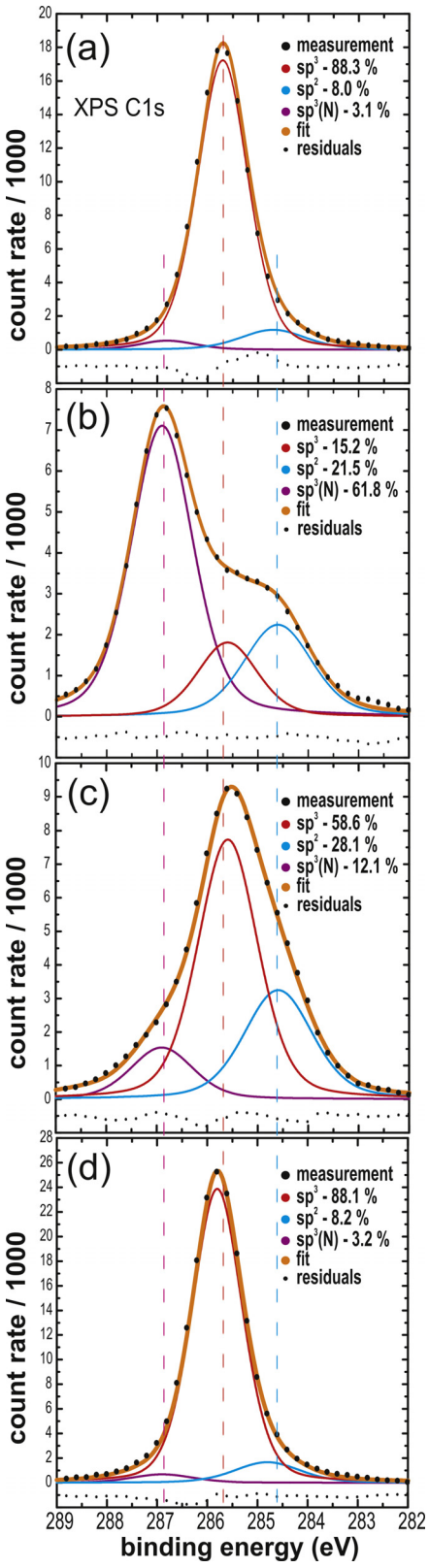

Figure 5. XPS C 1s peak deconvolution for the diamond sample in different preparation states. The energies given are the peak positions for the three most important spectral contributions as obtained by the fit, including residuals revealing the difference between measured and fit data points. (a) Pristine surface – sp^2 284.7 eV, sp^3 285.7 eV, sp^3(N) 286.9 eV; (b) nitrogen implanted surface – sp^2 284.6 eV, sp^3 285.6 eV, sp^3(N) 286.9 eV; (c) surface after etching in oxygen for 12 h at 790 °C sp^2 284.6 eV, sp^3 285.6 eV, sp^3(N) 286.9 eV; (d) surface after wet chemical etching and flashing to 790 °C – sp^2 284.8 eV, sp^3 285.8 eV, sp^3(N) 286.9 eV.

working mode, a line shape GL (30) with $m = 0.7$ yields the best fitting results. The starting values for the width ΔE and position E_0 are determined differently. For the peak width of the sp^3 component, a value derived from the initial untreated diamond surface is used while for fitting the sp^2 component, the width of the C line in spectra measured in our system on a clean graphite sample is used. For the sp^3(N) component, a larger peak width is used to account for a spread in local properties. The energetic position of sp^3 carbon depends on the doping of diamond where values ranging from 284 eV to 286.7 eV are reported in the literature [31,39]; we start our fit with 285.7 eV, the position found for the pristine diamond sample. The position of the sp^3(N) peak depends on the nitrogen doping level and varies between about 284.2 eV and 288.5 eV [40], we start with a value of 286.9 eV yielding the best fit for the preparation state with most implanted nitrogen present. The sp^2 carbon peak positions reported in literature [41,42] vary from 284.4 eV to 284.7 eV; we adopt a starting value of 284.7 eV measured for graphite in our system. When performing the fit, we fix the distance between sp^3 and sp^2 peak positions to 1 eV to reduce the number of free parameters. The fit procedure is based on routines from the CasaXPS software and we obtained best results by a manual variation of fit parameters. The final peak positions yielded by the fit exhibit only insignificant variations from the starting values and the same values are found for the surface in all states of preparation. This indicates the robustness of the experiments against charging and the integrity of data analysis.

As a further check, we consider three additional spectral components, namely oxidation related peaks C—O (1), C—O (2) and the tail of the π–π^* loss energy peak. Peaks related to either C=O or C—O—C bridge bonding [43] appear at 287.5 eV and 288.5 eV, while the feature related to the π–π^* transition is shifted by about 6 eV relative to the sp^2 peak [41,42,44,45]. However, none of the many trials in improving the fit by the inclusion of additional components yields a significant contribution and the clear conclusion is that the additional peaks contribute only by 1–2% to the total intensity. Therefore, they are not shown in the spectra.

The deconvolution result for the C 1s peak of the pristine surface is shown in Figure 5(a) and yields a strong contribution from sp^3 (88%), a ten times smaller contribution of sp^2 (8%) and a minute amount of sp^3(N) (3%) as expected for a high quality diamond sample with a well-prepared surface. The dramatic impact of nitrogen ion implantation is seen in the C 1s line shape analysis shown in Figure 5(b). The dominating peak is now the sp^3(N) component at 286.9 eV (62%), however, also the sp^3 peak presumably originating from deeper layers exhibits a significant intensity (15%). Surface damage due to the ion impact as discussed above is here evident from the strongly increased sp^2 peak (22%).

To remove the implanted nitrogen, the sample is etched in oxygen at a partial pressure of 1.33×10^{-7} mbar while the sample is kept at a temperature of 790 °C. Etching is accomplished in many steps of 2 h with an overall annealing time of 27 h. After 20 h, the temperature is increased to 830 °C and for the last 2 h, the temperature is set to 890 °C. Figure 5(c) shows the C 1s peak measured after 12 h of etching in oxygen. The main feature is again the sp^3 peak (59%) at 285.6 eV while the sp^3(N) contribution is dramatically decreased (12%). The increased intensity of the sp^2 peak (28%) points to a further degradation of the surface by the oxygen etching procedure. Further annealing in oxygen yields the expected complete removal of nitrogen and a complete conversion of sp^3 to sp^2 bonding within the XPS sampling depth (result not shown). In several further experiments with a variation of the oxygen partial pressure and annealing temperatures, we never succeeded in maintaining a high fraction of sp^3 bonding while effectively etching the surface.

To restore the surface with a high sp^3 phase purity, we apply the final step of wet chemical etching with respective XPS results for C 1s shown in Figure 5(d). The peak position and shape is identical within the experimental and fit errors to the result of the pristine surface shown in Figure 5(a); we recover the surface in perfect phase purity and cleanliness.

4. Conclusions

Our results demonstrate the repetitive preparation of a diamond (1 0 0) surface with highest phase purity from the same diamond crystal. The surface stoichiometry is dominated by partial oxidation due to the final step of treatment in oxidizing acids. However, this termination could be changed by further treatment in other acids or by a plasma treatment. The study further demonstrates efficient etching of the surface in an oxygen atmosphere with the sample kept at an elevated temperature. We point out, however, that etching is demonstrated here for a surface that has been heavily damaged by a bombardment with energetic ions at a high flux; the etching efficiency may be different for a less damaged surface. The results presented here and further experiments we performed show that it is not possible to maintain a high level of sp^3 phase purity for a surface treatment involving annealing in vacuum or in an oxygen atmosphere. The high sp^3 content of the pristine diamond crystal can, however, fully be restored by wet chemical etching. By re-inserting into the vacuum and cleaning by mild heating, a clean diamond surface with perfect phase purity can be prepared.

Acknowledgement

The authors gratefully acknowledge financial support from the VolkswagenStiftung through the project Az. 86392 in the framework program ‘Integration of molecular components in functional macroscopic systems’.

References

[1] R.J. Epstein, et al., Nat. Phys. 1 (2005) 94.
[2] T.D. Ladd, et al., Nature 464 (2010) 45.
[3] J. Wrachtrup, PNAS 107 (2010) 9479.
[4] R. Chapman, T. Plakhotnik, Chem. Phys. Lett. 507 (2011) 190.
[5] J.V. Macpherson, Phys. Chem. Chem. Phys. 17 (2015) 2935.
[6] K.B. Holt, Phys. Chem. Chem. Phys. 12 (2010) 2048.
[7] S. Orlanducci, et al., Chem. Phys. Lett. 549 (2012) 51.
[8] R.S. Sussmann, CVD Diamond for Electronic Devices and Sensors, John Wiley & Sons, Ltd., 2009.
[9] J.A. Garrido, et al., Appl. Phys. Lett. 86 (2005) 073504.
[10] W. Dexters, et al., Phys. Chem. Chem. Phys. 17 (2015) 9619.
[11] Q. Yu, et al., Chem. Phys. Lett. 539 (2012) 74.
[12] S.A.O. Russell, et al., IEEE Electron Device Lett. 33 (2012) 1471.
[13] D.A.J. Moran, et al., IEEE Electron Device Lett. 32 (2011) 599.
[14] M.Y. Liao, et al., Phys. Rev. B 81 (2010) 033304.
[15] T. Teraji, et al., J. Appl. Phys. 105 (2009) 126109.
[16] K. Haenen, et al., J. Phys.: Condens. Matter 21 (2009) 364204.
[17] H.A. Girard, et al., Phys. Chem. Chem. Phys. 13 (2011) 11517.
[18] V.N. Mochalin, et al., Nat. Nanotechnol. 7 (2012) 11.
[19] A. Alhaddad, et al., Small 7 (2011) 3087.
[20] K.V. Purtov, et al., Nanoscale Res. Lett. 5 (2010) 631.
[21] S. Schaefer, et al., Solid State Sci. 10 (2008) 1314.
[22] W. Harneit, et al., Phys. Status Solidi B 233 (2002) 453.
[23] W. Harneit, Phys. Rev. A 65 (2002) 032322.
[24] R. Kalish, Quantum Information Processing with Diamond: Principles and Applications, Woodhead Publishing, 2014.
[25] M. Nimmrich, et al., Phys. Rev. B 81 (2010) 201403R.
[26] A. Gruber, et al., Science 276 (1997) 2012.
[27] I. Kusunoki, et al., Surf. Sci. 492 (2001) 315.
[28] W. Deferme, et al., Diamond Relat. Mater. 15 (2006) 687.
[29] K. Bobrov, et al., Appl. Surf. Sci. 196 (2002) 173.
[30] Y. Kawabata, J. Taniguchi, I. Miyamoto, Diamond Relat. Mater. 13 (2004) 93.
[31] L. Diederich, et al., Surf. Sci. 417 (1998) 41.
[32] P. John, et al., Diamond Relat. Mater. 11 (2002) 861.
[33] H. Estrade-Szwarckopf, Carbon 42 (2004) 1713.
[34] S. Pezzagna, et al., New J. Phys. 13 (2011) 035024.
[35] D.N. Belton, S.J. Schmieg, J. Vac. Sci. Technol. A 8 (1990) 2353.
[36] J.I.B. Wilson, J.S. Walton, G. Beamson, J. Electron Spectrosc. Relat. Phenom. 121 (2001) 183.

[37] S. Kaciulis, Surf. Interface Anal. 44 (2012) 1155.
[38] S. Evans, Surf. Interface Anal. 17 (1991) 85.
[39] S. Ferro, M. Dal Colle, A. De Battisti, Carbon 43 (2005) 1191.
[40] J. Chastain, J.F. Moulder, Handbook of X-ray Photoelectron Spectroscopy: A Reference Book of Standard Spectra for Identification and Interpretation of XPS Data, Physical Electronics Division, Perkin-Elmer Corporation, 1992.
[41] F.R. McFeely, et al., Phys. Rev. B 9 (1974) 5268.
[42] P.A. Brühwiler, et al., Phys. Rev. Lett. 74 (1995) 614.
[43] S. Skokov, B. Weiner, M. Frenklach, Phys. Rev. B 49 (1994) 11374.
[44] V.S. Smentkowski, et al., Surf. Sci. 330 (1995) 207.
[45] R. Graupner, et al., Diamond Relat. Mater. 3 (1994) 891.